HHS Public Access

Author manuscript

Eur J Med Chem. Author manuscript; available in PMC 2020 January 01.

Published in final edited form as:

Eur J Med Chem. 2019 January 01; 161: 310–322. doi:10.1016/j.ejmech.2018.10.034.

Bimetallic titanocene-gold phosphane complexes inhibit invasion, metastasis, and angiogenesis-associated signaling molecules in renal cancer

Benelita T. Elie[a,b], **Jacob Fernández-Gallardo**[a], **Natalia Curado**[a], **Mike A. Cornejo**[a], **Joe W. Ramos**[e], and **María Contel**[a,b,c,d,e]

[a]Department of Chemistry, Brooklyn College, The City University of New York, Brooklyn, NY, 11210, US.

[b]Biology, The Graduate Center, The City University of New York, 365 Fifth Avenue, New York, NY, 10016, US.

[c]Biochemistry, The Graduate Center, The City University of New York, 365 Fifth Avenue, New York, NY, 10016, US.

[d]Chemistry PhD Programs, The Graduate Center, The City University of New York, 365 Fifth Avenue, New York, NY, 10016, US.

[e]Cancer Biology Program, University of Hawaii Cancer Center, University of Hawaii at Manoa, Honolulu, USA.

Abstract

Following promising recent *in vitro* and *in vivo* studies of the anticancer efficacies of heterometallic titanocene–gold chemotherapeutic candidates against renal cancer, we report here on the synthesis, characterization, stability studies and biological evaluation of a new titanocene complex containing a gold-triethylphosphane fragment [(η-C_5H_5)$_2$TiMe(μ-mba)Au(PEt_3)] (**4**) Titanofin. The compound is more stable in physiological fluid than those previously reported, and it is highly cytotoxic against a line of human clear cell renal carcinoma. We describe here preliminary mechanistic data for this compound and previously reported [(η-C_5H_5)$_2$TiMe(μ-mba)Au(PPh_3)] (**2**) Titanocref which displayed remarkable activity in an *in vivo* mouse model. Mechanistic studies were carried out in the human clear cell renal carcinoma Caki-1 line for the bimetallic compounds [(η-C_5H_5)$_2$TiMe(μ-mba)Au(PR_3)] (PR_3 = PPh_3 **2** Titanocref and PEt_3 **4** Titanofin), the two monometallic gold derivatives [Au(Hmba)(PR_3)] (PR_3 = PPh_3 **1** cref; PEt_3 **3**

*Corresponding Author M.C: MariaContel@brooklyn.cuny.edu; phone, (+1) 7189515000 (x2833).

Conflict of interest

The authors declare no conflict of interest for this article.

Appendix A. Supplementary Data. NMR, IR and UV-vis spectra of new compounds **3** and **4**; stability studies of compound Titanofin (**4**) by NMR and UV-vis spectroscopy; crystallographic data for compound **3** (fin); complete cytotoxicity and viability profile for bimetallic Titanocref (**2**), Titanofin (**4**) and for monometalic cref (**1**), fin (**3**) and Auranofin; selected targets found from the Proteome Profiler Human Protease Array assay for compounds **1**-**4** and Auranofin.

fin), titanocene dichloride and Auranofin as controls. These studies indicate that bimetallic compounds Titanocref (**2**) and Titanofin (**4**) are more cytotoxic than gold monometallic derivatives (**1** and **3**) and significantly more cytotoxic than titanocene dichloride while being quite selective. Titanocref (**2**) and Titanofin (**4**) inhibit migration, invasion, and angiogenic assembly along with molecular markers associated with these processes such as prometastatic IL(s), MMP(s), TNF-α, and proangiogenic VEGF, FGF-basic. The bimetallic compounds also strongly inhibit the mitochondrial protein TrxR often overexpressed in cancer cells evading apoptosis and also inhibit FOXC2, PECAM-1, and HIF-1α whose overexpression is linked to resistance to genotoxic chemotherapy. In summary, bimetallic titanocene-gold phosphane complexes (Titanocref **2** and Titanofin **4**) are very promising candidates for further preclinical evaluations for the treatment of renal cancer.

Graphical Abstract

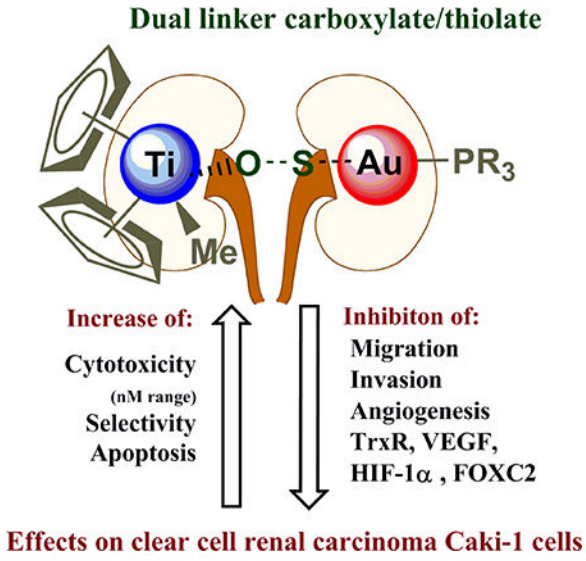

Keywords

Bimetallic; titanium-gold; renal cancer; mechanisms; metastasis; angiogenesis

1. Introduction

The potential of heterometallic compounds in medicinal chemistry and most particularly in cancer therapy has been recently described [1]. A single molecule with two or more distinct biologically active metallic centers can potentiate oncotherapeutic efficacy [2]. This may derive from synergism (combined action of the different metals) or cooperation (beneficial change in the physicochemical properties) between the two metal entities. In the past eight years a number of heterometallic compounds have been reported as anticancer agents [1–30]. However there are very few publications reporting the comparison of anticancer properties of heteronuclear compounds to that of their monometallic fragments (alone or in combination) [1,3,15,25–30]. Our group has focused on heterometallic compounds with gold fragments as one of the metallic centers. Gold(I) compounds bearing lipophilic ligands

such as phosphanes (PR_3) and N-heterocyclic carbenes (NHC) have displayed significant antitumor, antimicrobial and antiparasitic effects mostly by inhibition of the thioredoxin/thioredoxin reductase Trx/TrxR systems [31–33]. In this context, we have recently reported on the preparation of complexes containing titanocenes [24–28] [$TiCp_2$] or ruthenium(II) arene derivatives [29,30] [Ru(p-cymene)Cl_2(dppm)] and gold(I)-phosphane or gold(I)-NHC fragments (**2**, **a** and **b** in Chart 1) and their potential as chemotherapeutics against renal, colorectal and prostate cancers. Titanocenegold derivatives containing gold-phosphane fragments (such as compound **2**, Titanocref) shrank tumors by 67% in a xenograft mouse model of renal carcinoma after 21 days of treatment, and that with low systemic toxicity [26].

Preliminary mechanistic studies indicated that these compounds achieve toxicity through mechanisms different than that of cisplatin as is the case for many other metallodrugs [25,26,30]. The Ti-Au derivatives studied did not bind to DNA, however they were excellent inhibitors of protein kinases such as p90-RSK, AKT, and MAPKAPK [26], and thioredoxin reductase [26,27] (the inhibition occurred for both isolated kinases and in renal or prostate cancer cell lines). We report here on the synthesis and characterization of a new bimetallic titanocene containing a gold-phosphane fragment ($AuPEt_3$) that is also present in the drug Auranofin (AF). AF has been used in the clinic for the treatment of rheumatoid arthritis [34] but it is currently being investigated in clinical trials in cancer as a potential anticancer chemotherapeutic [35–38]. It has been described recently that human serum albumin adducts of $[AuPEt_3]^+$ have inhibited T cell proliferation at nanomolar doses [39]. It has also been reported that the cytotoxic properties of AF on colorectal cancer cells and the inhibition of purified TrxR depend solely on the $[AuPEt_3]^+$ fragment, and that the presence of the thiosugar moiety does not contribute to the pharmacologic efficacy of AF [33]. We have named the new Ti-Au compound [(η-C_5H_5)$_2$TiMe(μ-mba)Au(PR_3)] (**4**) Titanofin (Equation 1).

Here we report comparative *in vitro* mechanistic evaluation of the efficacy of two bimetallic [(η-C_5H_5)$_2$TiMe(μ-mba)Au(PR_3)] compounds (PR_3 = PPh_3 **2** [26], PEt_3 **4**) with that of AF and the monometallic gold compounds [Au(Hmba)PR_3] (PR_3 = PPh_3 **1** cref [26], PEt_3 **3** fin). All compounds are depicted in Chart 1 or in Equation 1. We studied their cytotoxicity, type of cell death induction, cell cycle disruption as well as anti-migratory and anti-angiogenic properties along with inhibitory effects on 84 markers of oncological interest. We have recently reported on the *in vitro* (caki-1 cancer cells) mechanism of action of a ruthenium-gold derivative in which we also used AF as control in a number of similar experiments [30].

2. Results and discussion

2.1. Synthesis and characterization

The new compound [(η-C_5H_5)$_2$TiMe(μ-mba)Au(PEt_3)] (**4**) Titanofin, is obtained in high yield (87%) in a similar manner to that of [(η-C_5H_5)$_2$TiMe(μ-mba)Au(PPh_3)] (**2**) [26] by reaction of [Au(Hmba)(PEt_3)] (**3**) and [(η-C_5H_5)$_2$$TiMe_2$] (Equation 1). The new compounds were obtained in moderate (**3**) or high (**4**) yields as white (**3**) or orange (**4**) solids, respectively. The synthesis and characterization details are provided in the experimental and NMR and IR spectra are provided in the SI.

Crystals suitable for X-diffraction were obtained for new compound [Au(Hmba)(PEt_3)] (**3**) fin. As for previously described phosphane [Au(Hmba)(DPPF)] [27] and N-heterocyclic carbene [Au(Hmba)(IMes)] [27] compounds with the Hmba ligand, the individual dimeric units (SI, figure S19) form chains which show hydrogen bonding at one end (Figure 1). Bond distances and angles are depicted in Table 1.

In this case, the monomeric molecules are linked by intermolecular gold-gold interactions (3.0678(4) Å) not present in similar compounds described by us and others (S19) [25,26]. Such interactions giving rise to oligomers (Au-Au distances at 2.8–3.3 A˚, well below the sum of the van der Waals radii of ca. 3.6 A˚) are common in gold chemistry and are due to the effect of aurophilicity [40,41]. The resulting dimeric units are linked by O-H intermolecular contacts (with the corresponding O or H from a second dimeric unit). The environment of the gold atoms is close to linear [P-Au-S 177.32(3)] (Figure 1). The ORTEP drawing and crystal and refinement data for this structure are provided in the SI.

The structure of bimetallic complex **4** depicted in Equation 1 has been proposed on the basis of NMR, IR and UV-vis spectroscopy, mass spectrometry, and elemental analysis (see experimental section and SI). The difference between the symmetric and antisymmetric stretching bands in the solid-state IR spectra of compound **4** (Titanofin) is 377 cm^{-1}, i.e. larger than 200 cm^{-1}, which points out that the carboxylate group is bonded to the titanium center in a monodentate fashion as we found previously for Titanocref (**2**) [26] and derivatives where the phosphane is replaced by heterocyclic (NHC) carbenes [27].

The stability of Titanofin **4** was evaluated by $^{31}P\{^1H\}$ and ^1H NMR spectroscopy in DMSO-d_6, 3:2 DMSO-d_6/PBS-D_2O and UV−vis spectroscopy in a 1:99 DMSO/PBS solution (NMR and UV-Vis spectra corresponding to stabilities studies are included in the SI). Titanofin (**4**) resulted more soluble than Titanocref (**2**) in mixtures DMSO/PBS. While the half-life for Titanocref (**2**) was in neat DMSO-d_6 was 8 hours, the half-life of new Titanofin (**4**) was 24 h (three times higher). In addition, Titanofin resulted soluble in mixtures DMSO:D_2O (3:2) and the stability in these solutions was higher (4 days). Both Titanocref (**2**) and Titanofin (**4**) are soluble in DMSO:PBS (1:99) in the micromolar range (necessary for the biological assays).

2.2. Cytotoxicity, Selectivity, Cell Death and Cell Cycle Arrest

The cytotoxicity of the bimetallic [(η-C_5H_5)$_2$TiMe(μ-mba)Au(PR_3)] (PR_3 = PPh_3 **2** Titano-CREF and PEt_3 **4** Titanofin), the two monometallic gold derivatives [Au(Hmba)(PR_3)] (PR_3 = PPh_3 **1** cref; PEt_3 **3** fin), and monometallic titanocene dichloride was evaluated. For comparative purposes, the cytotoxic profile of Auranofin was also determined. In this assay, human clear-cell renal carcinoma Caki-1 cells and non-tumorigenic human fetal lung fibroblasts (IRM-90) were incubated with the compounds **1**-**4**, Auranofin or titanocene dichloride for 72 hours. The results are summarized in Table 2. In the supplementary information section there is a more complete table that includes IC_{50}, IC_{20}, and IC_{10} values at 72 hours and IC_{50} and IC_{20} values at 24 hours (Table S3).

The heterometallic compounds are considerably more toxic to the renal cancer cell line (Caki-1 cells) than titanocene dichloride and Auranofin (in the sub-micromolar range as already reported for Titanocref for different renal cancer cell lines [26,27]).

In addition, Titanocref **2** is far more toxic in the nanomolar range than the monometallic gold compound **1** cref on these cells. Titanofin **4** is three times more toxic than the monometallic compound with PEt_3 (**3**) fin. This supports the hypothesis that the presence of two biologically active metals improves cytotoxicity. Importantly, both heterometallic compounds are more selective to renal cancer cells than Auranofin or the monometallic gold compounds, especially Titanocref **2.**

In addition to the IC_{50} at 72h, we also assessed the IC_{50} after 24h of incubation (Table S3 in SI). Because we sought to determine the changes in behavior as well as their associated molecular signaling it was essential that the cells be alive, therefore we used concentrations at which we know that after 72h incubation 80% (IC_{20}) or 90% (IC_{10}) of the cells would be viable (see Table S3 in SI). Some assays were carried out after 24h of incubation with the 72h IC_{20} which is the lowest dose at which we saw after 24h detectable changes in expression levels of the proteins we interrogated (Table S3 in SI). The relevance of the 24h IC_{50} evaluation is to demonstrate that the 72h IC_{20} of the compound do not induce significant cytotoxicity after 24h incubation.

Following the evaluation of the cytotoxicity of bimetallic Titanocref (**2**), Titanofin (**4**) and monometallic gold Auranofin, we proceeded to evaluate how the cells died. For this assay Caki-1 cells were incubated with the indicated compound at the IC_{50} concentration for 72 hours. We observed that all the compounds induce apoptosis to some degree at their IC_{50} concentration. For the Ti-Au compounds Titanocref (**2**) and Titanofin (**4**) (at nanomolar concentration) 58% and 76% of cells die by apoptosis (Figure 2).

Auranofin and other gold (I) compounds are known to induce apoptosis in several cancer cell lines [35,42], TDC also induces apoptosis albeit at much higher concentrations than the aforementioned compounds [43]. Thus the apoptotic phenotype of bimetallic Titanofin and Titanocref may be due to the presence of both, the Ti and Au fragments.

Next we evaluated the effects of bimetallic Titanocref (**2**), Titanofin (**4**) and monometallic Au Auranofin on cell cycle arrest.

Titanocref (**2**) and Titanofin (**4**) decreased G_1/G_0 by 32% and 33% respectively and increased the G_2/M population by 38% and 36% respectively DMSO compared to control. Auranofin increased G_1/G_0 by 27% and induced an arrest of 76% of the cell population at G1/G0 (as observed recently by us [30]), while also generating a peak at $SubG_1$ in 20% of the cells arrest consistent with apoptosis. This suggests that the Auranofin induced complete G_1/G_0 arrest, as has already been reported for other cells lines treated with AF [44–48], or other anti-inflammatory drugs [49]. The cell cycle shift of Titanocref (**2**) and Titanofin (**4**) are strikingly similar to each other and unlike that of Auranofin suggesting that perhaps the Ti moieties account in part for the distribution in G2/M and the prevent the complete switch to G_1/G_0 observed with Auranofin.

In view of all results obtained and the very high concentration needed of TDC to observe cytotoxic effects, we decided not to explore the effects of titanocene dichloride in Caki-1 cells any further.

2.3. Inhibition of migration and invasion

The increased local cell migration and later the distal invasion seen in advanced tumors are hallmarks of metastasis [50,51]. We therefore evaluated the anti-migration and anti-invasive properties of bimetallic Titanocref (**2**), Titanofin (**4**) and monometallic gold cref (**1**), fin (**3**) and Auranofin. The effect of (IC_{20}) the compounds on migration was determined using a wound-healing 2D scratch assay on a collagen-coated plate (Figure 3A). We chose the IC_{20} because it was determined that at that concentration about 80% of the cells (78% ± 2.31 depending on the compound) are alive. Migration is quantified by measuring the space in the wound gap that is occupied by cells 24h after treatment. We observed that heterometallic Titanocref (**2**) and Titanofin (**3**) as well as Auranofin significantly reduced migration by 89%, 83% and 81% respectively. Gold monometallic cref (**1**) and fin (**3**) inhibit migration to a lesser degree 40% and 33% respectively. While the cytotoxicity and apoptotic properties of Auranofin on different cancer cell lines are well known [35], the efficacy of Auranofin as an anti-migratory and perhaps anti-metastatic compound was unexpected and has only been recently reported by us [30]. All the compounds studied interfere with invasion and follow a similar trend as that of migration with Auranofin and Ti-Au compounds being most effective (Figure 3B). There is a clear trend that the monometallic gold compound fin (**3**) is a better inhibitor of invasion than cref (**1**), while their inhibition of migration is similar. This may be because proteolysis is necessary for the cells to infiltrate though the 3D matrix, but is not needed for 2D migration. Indeed fin (**3**) which is a better inhibitor of invasion is also a stronger inhibitor or MMP-9 and MMP-2 (see next sections) which are proteolytic agents known to be key players in migration and metastasis. As explained above, the most efficient compounds in these experiments were bimetallic Titanocref (**2**) and Titanofin (**4**).

2.4. Inhibition of angiogenesis

Neovascularization plays an essential role in tumor malignancy. We chose to examine the formation of tube-like structures by HUVEC cells in an extracellular matrix as an *in vitro* model [52] to assess the potential perturbation of angiogenesis is the most effective and potent bimetallic Ti-Au Titanocref (**2**), Titanofin (**4**) and Auranofin.

In this assay, the endothelial tube formation of Human umbilical vein endothelial cells (HUVECs) on an ECM-like matrix was determined as a function of length of the uninterrupted tubes (TL), and number of branching point or nodes in the tubes (TN) (Figure 4). The number of tubes and nodes was counted using Image-J with the Angiogenesis plugin. The greater the inhibition of tube formation, that is the lower length of tube (TL) and the lower the number of nodes (TN) the higher the anti-angiogenic properties of a compound.

All three compounds bimetallic Titanocref (**2**) and Titanofin (**4**) as well as control Auranofin induce similar disruption in tube integrity with an average of 50% in disruption tube length (TL) and 45% disruption in tube node (TN) formation. Disruption in vascular formation is a

key attribute of many anti-angiogenic compounds and can prevent tumor growth and hinder metastasis. Limiting a tumor's access to viable vasculature serves to deprive the tumor of nutrients for growth and an exit avenue through which it can escape for metastasis.

2.5. Inhibition of targets associated to cancer cisplatin resistance, metastasis and angiogenesis

2.5.1. Inhibition of Thioredoxin Reductase—Changes in intracellular anti-oxidant states are a distinctive feature of many chemo-resistant cancers. Overexpression of thioredoxin reductase (TrxR), an enzyme that controls intracellular redox state, is a critical condition for the survival of cisplatin-resistant cancer cells. Furthermore, TrxR overexpression has been causally linked to increased angiogenesis and therefore TrxR has become a salient therapeutic target [9,30,44,53–56]. We previously reported on the significant inhibition of TrxR in Caki-1 cells by Auranofin [26] and heterometallic titanocene-Au [26,27] and Ru-Au complexes [29,30]. We here measured the activity of (TrxR) in Caki-1 cells, following incubation with bimetallic Ti-Au Titanocref (**2**), Titanofin (**4**) and monometallic Au cref (**2**), fin (**3**) and Auranofin as a positive control (Figure 5). After 72 h of incubation Caki-1 TrxR activity is significantly reduced by Auranofin (86%), after 24h of incubation there was not a significant change [26,30]. After 72 h of incubation the inhibition of TrxR by the bimetallic Ti-Au Titanocref (**2**) and Titanofin (**4**) is very similar (Titanocref, 87%; Titanofin 79%). The inhibition is larger than the also strong inhibition displayed by monometallic gold compounds cref (**2**) and fin (**3**) of 54% and 57% respectively.

2.5.2. Inhibition of VEGF—Vascular endothelial growth factor (VEGF) is the key mediator of tumor angiogenesis through its up-regulated by oncogene and growth factors expression [57–59]. For solid tumors to grow beyond 0.5 cm in diameter, denovo angiogenesis is required for the delivery of nutrients and oxygen to the tumor site [49,57,58]. Therefore, VEGF along with other key growth factors produced by tumors in orchestrate an 'angiogenic switch', wherein vasculature is formed through and around the tumor, facilitating hyperproliferation and exponential growth [60]. Thus, given the significant tumor promoting capacities of VEGF we sought to assess whether or not its expression is affected by Ti-Au Titanocref (**2**), Titanofin (**4**) and monometallic Au cref (**2**), fin (**3**) and Auranofin on VEGF. We found that VEGF secretion is inhibited by both bimetallic Ti-Au Titanocref (**2**), Titanofin (**4**) and Auranofin after 72h incubation with IC_{20} of each compound (41% (**2**), 59% (**4**) and 55% (**AF**) reduction respectively), while for monometallic Au cref (**2**) and fin (**3**) there was no significant inhibition of VEGF secretion with it being 22% and 17% respectively, no significant change was observed after 24h incubation with IC_{20} of each compound. In this case the strong inhibition of VEGF could be correlated to the anti-angiogenic effects we found. VEGF is known to be a key regulator of angiogenesis and its downregulation is often correlated with reduced angiogenesis.

2.5.3. Inhibition of Cytokines (TNF-α and interleukins)—TNF- α (Tumor necrosis factor alpha) which is produced in immune and tumor cells plays a central role in inflammation, apoptosis, and cancer progression. Cell surface TNF-α can induce lysis in tumor cells or surrounding cells which induce the necrosis-like death phenotype. TNF-α can

bind to its receptor to induce apoptosis. TNF-α has bivalent capacities with pro— and anti—tumorigenic profiles and thus is of great interest in the development of anti-cancer drugs [61–63]

Interleukins (IL) are a class inflammatory cytokines known to be linked to metastasis when overexpressed in a number of epithelial breast, lung and kidney tumors [64–67]. Some members of the ILs family have been reported to stimulate tumor growth and metastasis via a number of proteolytic interactions and through control of several MMPs expression and the expression of proangiogenic proteins such as VEGF [59,67,68]. We studied the inhibition of ILs by bimetallic compounds Ti-Au Titanocref (**2**), Titanofin (**4**) and monometallic Au compounds cref (**1**), fin (**3**) and Auranofin after 72 hour of incubation at IC_{20} concentrations, we chose the 72h timepoint because no significant effect was observed after 24h of incubation with the same concentrations (Figure 6B). We found that the bimetallic compounds, gold monometallic compounds and auranofin inhibited IL-6 expression almost completely. Auranofin and Titanocref (**2**) also inhibited IL-5 expression while the inhibition by Titanofin (**4**) was more modest (89% Titanocref (**2**), 59% Titanofin (**4**) and 88% Auranofin). Auranofin was a better inhibitor for IL-8 while both bimetallic compounds Titanocref (**2**) and Titanofin (**4**) were much better IL-4 and IL-17A inhibitors. Titanocref (**2**), Titanofin (**4**) and monometallic Au cref (**2**) and fin (**4**) are particularly strong inhibitors of IL-17A. Because IL-17A expression is associated with ER(−) and triple negative tumor hyper proliferation and poor prognosis in breast cancer, IL-17 inhibitors are of clinical interest. Also, IL-17 promotes cancerous cell survival and invasiveness as well as angiogenesis. Auranofin, as previously reported, inhibits IL-6 [48], but we have observed that it also inhibits expression of IL-5 and IL-8 [30], all key players in inflammatory signaling. IL inhibitors are of further interest because they are known inducers of MMPs which are critical in metastasis [64,65,67].

Inhibition of matrix metalloproteases

Matrix metalloproteinases (MMPs) are a family of zinc-dependent extracellular remodeling endopeptidases that play a critical role in tumor growth and the complex processes of invasion and metastasis through proteolytic degradation of ECM, modifications of the cell-cell, cell-ECM communication. Also, several MMPs have been shown to promote angiogenesis [60,68–70]. Matrix metalloproteinase inhibitors (MMPIs) have been developed and continue to be explored as viable therapeutic regiments to curb cancer progression [68,69,71]. The several members of the MMP family proteolytic factors are drive tumor induced inflammation signaling and angiogenesis most often in cooperation with members of the IL family [65,67,72,73]. We studied the inhibition of several MMPs of oncological interest (MMP-1, MMP-2, MMP-3, MMP-7, MMP-8, MMP-9) by bimetallic Ti-Au Titanocref (**2**), Titanofin (**4**), and monometallic Au cref (**2**), fin (**3**) and Auranofin. The protein expression of all the selected MMPs are inhibited by the bimetallic compounds except MMP-2 which is most inhibited by the monometallic compounds. For MMP-3 both the bimetallic and monometallic compounds achieve inhibition greater than 50%. The inhibition of MMP-7 is significant and equally inhibited by the bimetallic compounds while the monometallic compounds cause no inhibition (Figure 7). Auranofin [30] and Titanofin

(**4**) (to a slightly higher degree) inhibit the expression of MMP-9 while Titanocref (**2**) and the monometallic Au cref (**2**) and fin (**3**) do not have much of an effect.

It is evident from the changes in expression we have observed as a result of treatment with Titanocref (**2**), Titanofin (**4**) and monometallic Au cref (**2**), fin (**3**) and Auranofin that while bimetallic compounds are most often more effective inhibitors than monometallic compounds, the latter do have a non-negligible IL(s) and MMP(s) inhibitory profile rendering them promising anti-cancer candidates (see fin **3**).

Owing to the fact that there is limited understanding of the pathways by which metallodrugs achieve efficacy, we performed for 72h at IC_{20} a protein expression screen of our compounds' effects on eighty-four cancer-related proteins. We chose the 72h timepoint because no significant effect was observed after 24h 72h at IC_{20} prior similar assay. From this screen we identified that our compounds had significant effect on nine markers of oncological interest in addition to the fourteen reported earlier in the paper. A salient point arose from our analysis, there seems to be some stratification of markers that are affected by the bimetallic and not the monometallic compounds and vice versa. This stratification represented in a heat map (Figure 7) warrants further exploration. Heat maps are two-dimensional representations of a data set from which one seeks to extract patterns between features such as treatment type for example. The protein expression level values can be arranged using stratification allowing for an informative visual summary.

In an attempt to determine if there is any clear pattern in the inhibition of protein of oncological for bimetallic compounds we made a heat map (Figure 7) including bimetallic Ti-Au (Titanocref **2** and Titanofin **4**) and monometallic Au (cref **1** and fin **3**) as well as Auranofin (used as control in all studies described here).

Markers whose levels vary significantly ($p < 0.05$) between at least two treatment groups (Titanocref **2**, Titanofin **4**, cref **1**, fin **3** and Auranofin) are projected on the heat map and used for clustering. The data plotted is reported in bar graph form in figures 5 and 6 and S20 (In SI). In the heat map (Figure 7) there are seven additional markers of interest in cancer progression that were inhibited by either bimetallic, monometallic or both classes of compounds that were not discussed earlier in the text. The degree of inhibition can be appreciated in the heat-map where DMSO serves as the 100% expression baseline.

From a protein array screen, we observed that the compounds interfered with the protein expression levels of CapG, ErbB2, FGF-basic, FOXC2, HIF-1α, Tenascin C and CD31/PECAM-1 all of which are involved in several aspects of tumor malignancy and their individual or collective overexpression correlate to poor prognosis. The capping proteins CapG and ErbB2 play a key role in breast and lung cancer invasion and is a predictor of poor outcome [74–76]. Basic fibroblast growth factor (FGF-basic) is known to stimulate angiogenesis directly driving up the proliferation, migration and overall survival of tumors [77–79]. The inhibition of Forkhead box protein C2 (FOXC2) is reported to restore drug sensitivity in some cancer cells, and reinstate epithelial phenotype to metastatic cells [80,81]. While the cell-adhesion and signaling molecule PECAM-1 is known to modulate resistance to genotoxic chemotherapy such as cisplatin treatment [82].

High expression of Hypoxia-inducible factor 1-alpha (HIF-1α) also correlates to poor prognosis in several cancer types [83–85]. The extracellular matrix protein tenascin C is overexpressed in the invasive front of several cancer types during local invasion, and it is also associated with poor clinical outcome [86–88].

Along with the fifteen markers discussed earlier, the broad hitting range of inhibition of pro-tumorigenic signaling molecules by monometallic Au cref (**2**), fin (**3**) and more importantly by bimetallic Titanocref (**2**), Titanofin (**4**) is a testament to their great potential in inhibiting tumor progression on several fronts. Auranofin has also emerged as a significant inhibitor of a number of factors critical of tumor malignant progression and metastasis in human clear-cell renal carcinoma Caki-1 as exhibited throughout this body of work and that recently published by our group [30]. These findings are informative not only in guiding further rational design, but also on the merit that it adds mechanistic insights to an FDA approved drug that is actively being explored as a potential anticancer agent. Broadening our understanding of the mechanism by which Auranofin archive efficacy is a valuable contribution to the study of its potential as safe, readily available in the clinic and efficient anticancer agent.

What has become evident from our evaluations is that however effective the monometallic compounds might be, overall the bimetallic compounds are more potent and affect a broader spectrum of molecular targets and cellular behaviors than any single isolate monometallic as can be observed in the compounds inhibition of migration, invasion, angiogenesis as well as their inhibition of VEGF, MMP(s) and IL(s).

3. Conclusions

This study expands on the discovery of the high efficacy *in vitro* in a human clear-cell renal carcinoma cell line displayed by bimetallic titanocene-gold derivatives. One of the compounds (Titanocref) had been described as extremely efficacious *in vitro* and *in vivo* previously. In this study we include a more complete mechanistic view on Titanocref and on a second related compound (Titanofin) that contains the same gold-phosphane fragment as Auranofin. Comparisons were made with Auranofin as control and with the monometallic gold precursors necessary to prepare these bimetallic titanocene-gold derivatives. While we have used titanocene dichloride (TDC) as titanocene monometallic control, in some cases the high amounts (well over 100 micromolar) needed to observe effects have precluded us to use it for relevant comparisons in most assays. The bimetallic compounds Titanocref and Titanofin strongly inhibit migration, invasion, and angiogenic assembly along with molecular markers associated with these processes such as prometastatic IL(s), MMP(s), TNF-α and VEGF. Bimetallic titanocene-gold compounds have thus emerged as potential chemotherapeutics for renal cancer as they hinder three of the most harmful behaviors of the tumor microenvironment that is, local migration of tumor cells, their invasion into the vasculature for metastasis and the formation of de novo blood vessels through which cancerous cells can metastasize. We evaluated Auranofin and observed great similarities in efficacies to the bimetallic compounds in Caki-1 cells as an inhibitor of proliferation and hindering metastatic phenotypes. Auranofin also curbed expression of VEGF and IL(s).

Points of dissimilarity are that Auranofin induced cell arrest at G1/G0, while Titanocref and Titanofin induced arrest at G2/M.

These results along with those published for Titanocref *in vivo* warrant further efficacy, pharmacokinetic and histopathological studies and mechanistic exploration *in vivo* for bimetallic titanocene-gold derivatives. In addition, the relevant results found for Auranofin also warrant further exploration of this FDA approved agent for rheumatoid arthritis agent in renal cancer treatment.

4. Experimental

4.1. Chemistry

4.1.1. General and Instrumentation for the Characterization and Stability Studies of the New Compounds—

NMR spectra were recorded in a Bruker AV400 (^{1}H-NMR at 400 MHz, ^{13}C{^{1}H} NMR at 100.6 MHz and ^{31}P{^{1}H} NMR at 161.9 MHz. Chemical shifts (δ) are given in ppm using $CDCl_3$ as the solvent, unless otherwise stated. ^{1}H and ^{13}C NMR resonances were measured relative to solvent peaks considering tetramethylsilane = 0 ppm, and ^{31}P{^{1}H} NMR was externally referenced to H_3PO_4 (85%). Coupling constants *J* are given in hertz. IR spectra (4000 to 250 cm^{-1}) were recorded on a Nicolet 6700 Fourier transform infrared spectrophotometer on solid state (ATR accessory). Elemental analyses were performed on a Perkin-Elmer 2400 CHNS/O series II analyzer. Mass (MS) spectra (electrospray ionization, ESI) were performed on a Waters Q-Tof Ultima. Stability studies were performed in a Cary 100 Bio UV-visible spectrophotometer. The pH was measured in an OAKTON pH conductivity meter in 1:99 DMSO/H_2O solutions.

4.1.2. Synthesis—

All compounds involving titanium centers were prepared and handled with rigorous exclusion of air and moisture under a nitrogen atmosphere by using standard nitrogen/vacuum manifold and Schlenk techniques. Solvents were purified by use of a PureSolv purification unit from Innovative Technology, Inc. Titanocene dichloride and [AuCl(PEt_3)] were purchased from Aldrich, Auranofin was purchased from Strem and 4-mercaptobenzoic acid from TCI America Inc. and used without further purification. [Au(Hmba)(PPh_3)] [25], (**1**), [(η-C_5H_5)$_2$TiMe$_2$] [89], and [(η-C_5H_5)$_2$TiMe(μ-mba)Au(PPh_3)] [25,26], (**2**) Titanocref were prepared as previously reported.

[Au(Hmba)(PEt_3)] (3) fin.: H_2mba (0.245 g, 1.58 mmol) was dissolved in a solution of KOH (0.089 g, 1.58 mmol) in 20 mL of ethanol (16 mL) and water (4 mL) and was stirred for 20 minutes at room temperature. [AuCl(PEt_3)] was added to the solution afterwards, and the mixture was stirred for 2 hours. The solvents were removed under reduced pressure, and the residue was washed with water (3 × 2mL) and then diethyl ether (3 × 3 mL) to afford compound **3** as white powder in 69% yield (0.512 g). Anal. Calc. for $C_{13}H_{20}AuO_2PS$ (468.30): C, 33.34; H, 4.30; S, 6.85. Found: C, 33.04; H, 4.42; S, 6.40. ^{31}P{^{1}H} NMR ($CDCl_3$): δ 36.92. ^{1}H NMR ($CDCl_3$): δ 7.79 (2H, d, $^{3}J_{H\text{-}H}$ = 8.3 Hz, 2-C_6H_4), δ 7.60 (2H, d, $^{3}J_{H\text{-}H}$ = 8.2 Hz, 3-C_6H_4), δ 1.88 (6H, m, -C*H*$_2$CH$_3$), δ 1.25 (9H, dt, $^{3}J_{H\text{-}H}$ = 18.5, 7.6 Hz, -CH$_2$C*H*$_3$). ^{13}C{^{1}H} NMR ($CDCl_3$): δ 171.90 (s, C=O), δ 153.05 (s, 4-C_6H_4), δ 132.34 (s, 2-C_6H_4), δ 130.02 (s, 3-C_6H_4), δ 124.05 (s, 1-C_6H_4), δ 18.46, (d, $^{3}J_{C\text{-}P}$ = 33.3 Hz, -*C*H$_2$CH$_3$), δ 9.41 (s, -CH$_2$*C*H$_3$). IR (cm^{-1}): 2962 m,br (OH), 1668 s, 1578 s (ν_{asym} CO_2),

1325 m, 1292 vs (ν_{sym} CO_2), 1176 m, 1085 m, 760 m. pH **2** (5×10^{-5} M in 1:99 DMSO:H_2O) = 4.53.

[(η-C_5H_5)$_2$TiMe(μ-mba)Au(PEt_3)] (4) Titanofin.: [Au(Hmba)(PEt_3)] **2** (0.248 g, 0.53 mmol) was dissolved in tetrahydrofuran (10 mL) and dropwise added over a solution of Cp_2TiMe_2 (0.120g, 0.53 mmol) in toluene (5 mL) to yield a bright yellow solution that was stirred at RT until the methane release ended (1 hour). The solvents were then removed under reduced pressure and the crude washed with diethyl ether (3×10 mL). The bimetallic complex **4** that was isolated as a pale orange solid in 87% yield (0.303 g). Anal. Calc. for $C_{24}H_{32}AuO_2PSTi$ (660.10): C, 43.65; H, 4.88; S, 4.86. Found: C, 43.77; H, 4.99; S, 5.02. $^{31}P\{^1H\}$ NMR ($CDCl_3$): δ 37.23. ^1H NMR ($CDCl_3$): δ 7.49 (2H, d, $^3J_{H\text{-}H}$ = 8.4 Hz, 2-C_6H_4), δ 7.40 (2H, d, $^3J_{H\text{-}H}$ = 8.4 Hz, 3-C_6H_4), δ 6.26 (10H, s, C_5H_5), δ 1.87 (6H, dq, $^3J_{H\text{-}H}$ = 15.4, 7.7 Hz, -CH_2CH$_3$), δ 1.24 (9H, dt, $^3J_{H\text{-}H}$ = 18.5, 7.6 Hz, -CH$_2$CH_3), δ 0.97 (3H, s, CH_3-Ti). $^{13}C\{^1H\}$ NMR ($CDCl_3$): δ 172.03 (s, C=O), δ 148.85 (s, 4-C_6H_4), δ 132.20 (s, 2-C_6H_4), δ 129.81 (s, 3-C_6H_4), δ 128.81 (s, 1-C_6H_4), δ 114.69 (s, C_5H_5), δ 44.40 (s, CH_3), δ 18.46, (d, $^3J_{C\text{-}P}$ = 33.3 Hz, -CH$_2$CH$_3$), δ 9.41 (s, -CH$_2$$CH_3$). IR ($cm^{-1}$): 2960 w (Cp), 1631 vs (ν_{asym} CO_2), 1450 s (Cp), 1285 vs (ν_{sym} CO_2), 1168 m (Cp), 815 s (Cp). pH **3** (5×10^{-5} M in 1:99 DMSO:PBS buffer) = 7.30.

4.1.3. Crystal structure determination—Single crystals of **3** (pale yellow irregular fragment with approximate dimensions 0.18 × 0.40 × 0.45 mm) were mounted on a glass fiber in a random orientation. The X-ray intensity data were measured on a Bruker Smart Breeze CCD system equipped with a graphite monochromated Mo-Kα radiation (l=0.71073 Å) at 100(2) K, cooled by an Oxford Cryosystems 700 Series Cryostream. Space group assignments were based on systematic absences, E statistics and successful refinement of the structures. The structures were solved by direct methods with the aid of successive difference Fourier maps and were refined using the Bruker SHELXTL Software Package. All non-hydrogen atoms were refined anisotropically. Hydrogen atoms were assigned to ideal positions and refined using a riding model. These data can be obtained free of charge from The Cambridge Crystallographic Data Center via www.ccdc.cam.ac.uk/data_request/cif (CCDC 1579386) or in the Supplementary Information.

4.2. Biological Assays

4.2.1. Cell lines—Human renal cell carcinoma line Caki-1 was newly obtained for these studies from the American Type Culture Collection (ATCC) (Manassas, Virginia, USA) and cultured in Roswell Park Memorial Institute (RPMI-1640) (Mediatech Inc., Manassas, VA) media containing 10% Fetal Bovine Serum, certified, heat inactivated, US origin (FBS) (Gibco, Life Technologies, US), 1% Minimum Essential Media (MEM) nonessential amino acids (NEAA, Mediatech) and 1% penicillin–streptomycin (PenStrep, Mediatech). IMR90 (human fetal lung fibroblast) cells were purchased from ATCC (Manassas, Virginia, USA) and maintained in Dulbecco's modified Eagle's medium (DMEM) (Mediatech) supplemented with 10% FBS, 1% NEAA and 1% Penicillin Streptomycin. HUVEC (human umbilical vein endothelial) cells were obtained from ATCC and cultured in Medium 200PRF (Gibco, Life Technologies, US).

4.2.2. Cell Viability Analysis—The cytotoxic profile (IC_{50}) of bimetallic Ti-Au Titanocref (**2**), Titanofin (**4**) and monometallic Au cref (**2**), and fin (**3**) was determined by assessing the viability of Caki-1 and IMR90 control cells treated with the appropriate cultured medium containing 0.1 μM, 1 μM, 10 μM and 100 μM of compounds for 72h using the colorimetric cell viability assay PrestoBlue (Invitrogen). The cytotoxic profile of Auranofin and Titanocene dichloride (for comparative purposes) was also determined. All compounds were dissolved in DMSO except Cisplatin that was dissolved in H_2O with a final DMSO concentration of 1%. In the supplementary information section there is a more complete cytotoxic profile that includes IC_{50}, IC_{20}, and IC_{10} values at 72 hours and IC_{50} and IC_{20} values at 24 hours (Table S3).

4.2.3. Cell Death Assay—The cell death profile in Caki-1 cancerous cells cultured in the appropriate medium containing IC_{50} concentrations of bimetallic Ti-Au Titanocref (**2**), Titanofin (**4**) and monometallic Au cref (**2**), fin (**3**) and Auranofin for 24h was analyzed by flow cytometry stained with Annexin V (FITC) dye (Invitrogen). Staurosporine and Ionomycin treated cells were also stained with Annexin V dye and served as positive controls for apoptosis and cell death. FITC fluorescence intensity was detected with a flow cytometry analysis was conducted using a BD LSR II flow cytometer. $10*10^5$ events per sample were recorded. The flow cytometer was calibrated prior to use.

4.2.4. Cell Cycle Profile—The cell cycle profile in Caki-1 cancerous cells cultured in the complete RPMI medium containing IC_{20} concentrations of bimetallic Ti-Au Titanocref (**2**), Titanofin (**4**) and Auranofin for 24h was analyzed by flow cytometry wherein total DNA was stained with FxCycle Violet (FCV; DAPI) dye (Invitrogen). DAPI fluorescence intensity was detected with a BD LSR II flow cytometer and flow cytometry analysis was conducted using BD FACSDiva 8.0.2 $10*10^5$ events per sample were recorded. The flow cytometer was calibrated prior to use.

4.2.5. Cell Migration and Invasion Analysis—The anti-migratory profile of bimetallic Ti-Au Titanocref (**2**), Titanofin (**4**) and monometallic Au cref (**2**), and fin (**3**) Auranofin was assessed by *in vitro* scratch assay using Caki-1 cells treated with the appropriate cultured medium containing IC_{20} concentration of the compounds. The diluting agent (0.1% DMSO) served as positive control. Briefly, using 6-well collagen-coated plate cells were allowed to seed for 24h. After which, cells were serum starved for 4 hours, scratched by 200 μL tips. 24 hours after injury, cells were photographed using a Moticam camera mounted on a Zeiss microscope inverted microscope at 20X. The area invaded was measured in 5 randomly selected segments from each photo then averaged. Data were collected from two independent experiments performed.

The anti-invasion profile of bimetallic Ti-Au Titanocref (**2**), Titanofin (**4**) and Auranofin was assessed by transwell assay by determining the invasion of Caki-1 cancerous cells treated with the appropriate cultured medium containing IC_{20} concentration of the compounds. The diluting agent (0.1% DMSO) served as positive control. Briefly, Geltrex® a Reduced Growth Factor Basement Membrane Matrix (Invitrogen) is thawed and added to a 24-well transwell insert and solidified in a 37°C incubator for 30 minutes to form a thin gel layer.

Cell solution of $5*10^5$ cells in serum-free media is added on top of the Geltrex® coating to simulate invasion through the extracellular matrix. The insert was mounted into a well containing complete media. Invasion of cells toward the chemotactic gradient through the membrane to the underside was assessed after 24 hours when the membrane is fixed and stained with hematoxylin and eosin. Then the invaded cells were captured with a Moticam camera mounted on a Zeiss inverted microscope at 20X. Cell numbers were counted from 5 randomly selected field of view from each photo then averaged. Data were collected from at least two independent experiments performed.

4.2.6. Angiogenesis Analysis—The antiangiogenic profile of bimetallic Ti-Au Titanocref (**2**), Titanofin (**4**) and Auranofin were determined by assessing the endothelial tube formation of Human umbilical vein endothelial cells (HUVECs) treated with the appropriate cultured medium containing the above-mentioned compounds. Briefly, 96 well plates were coated with Geltrex®, Reduced Growth Factor Basement Membrane Matrix (Invitrogen) (50μl/well) and incubated at 37ºC for 30 minutes to allow gelation to occur. HUVECs were added to the top of the gel at a density of 6,000 cells/well in the presence or absence of Titanocref (**2**), Titanofin (**4**) or their monometallic controls (1 μM). The diluting agent (1% DMSO) served as positive control. Cells were incubated at 37ºC with 5% CO_2 for 24h and pictures were captured with a Moticam camera mounted on a Zeiss microscope inverted microscope at 10X. Quantification of tube formation was assisted by SCORE, a web-based image analysis system (S.CO BioLifescience). Tube formation quantified by Number of branching points (tube nodes, TN) and total length skeleton (tube length, TL). The data was obtained from the average of three wells per treatment condition.

4.2.7. Thioredoxin reductase activity assay—Caki-1 cells treated *in vitro* with IC_{50} concentrations of either Titanofin (**2**), Titanocref (**4**) the monometallic compounds cref (1), fin (**3**), and Auranofin or 0.1% DMSO were lysed after 24 hours of treatment. The lysate was then mixed with Thioredoxin Reductase Assay buffer, after 20 minutes incubation DTNB (5, 5′-dithiobis (2-nitrobenzoic) acid) was added TrxR levels were detected according to the manufacturer's instructions (Abcam kit, ab83463) using the BioTek Microplate Reader (BioTek U.S., Winooski, VT) at λ = 412 nm. Tests were done in duplicate. TrxR activity was calculated based on the linear amount of TNB produced per mg of total protein and adjusted for background activity from enzymes other than TrxR in the lysates.

4.2.8. VEGF Assay—Caki-1 cells treated *in vitro* with either IC_{20} concentrations of bimetallic Ti-Au Titanocref (**2**), Titanofin (**4**) and monometallic Au cref (**2**), and fin (**3**) and Auranofin or 0.1% DMSO were lysed after 72 hours of treatment, cell culture supernatant was collected and VEGF expression was sassessed by a VEGF human ELISA kit (100663 Abcam).

4.2.9. Cytokines—Caki-1 cells treated *in vitro* with either IC_{20} concentrations of bimetallic Ti-Au Titanocref (**2**), Titanofin (**4**) and monometallic Au cref (**2**), and fin (**3**) and Auranofin or 0.1% DMSO. After 72 hours of treatment, cell culture supernatant was collected, and interleukin expression was determined by Multi-Target ELISA array kit

(PathScan Cytokine Antibody Array Kit, Cell Signalling). The relative expression levels of the proteases were determined according to the manufacturer's protocol, and signal intensities were compared using HLImage^{++} software (R&D).

4.2.10. Protease array—Caki-1 cells treated *in vitro* with either IC_{20} concentration of bimetallic Ti-Au Titanocref (**2**), Titanofin (**4**) and monometallic Au cref (**2**), fin (**3**) and Auranofin or 0.1% DMSO were lysed after 72 hours of treatment. Before application to the array, protein concentration was determined by BCA. Then 150 ug of lysate was incubated for 24 h with the Proteome Profiler Human Protease Array Kit (ARY025, R&D Systems). The relative expression levels of the proteases were determined according to the manufacturer's protocol, and signal intensities were compared using HLImage^{++} software (R&D).

Supplementary Material

Refer to Web version on PubMed Central for supplementary material.

Acknowledgments

We thank the National Cancer Institute (NCI) and National Institute for General Medical Sciences (NIGMS) for grant 1SC1CA182844 (M.C.). N.C. thanks Fundación Alfonso Martín Escudero (Spain) for a postdoctoral fellowship. We are very grateful to Dr. Karen Hubbard for providing infrastructure and advice and Ciara Bagnall for her technical expertise in imaging and immunocytochemistry.

Abbreviations

ATCC	American Type Culture Collection
ADAM	a disintegrin and metalloproteinase
Auranofin	Gold(1+);(2S,3R,4S,5R,6R)-3,4,5-triacetyloxy-6-(acetyloxymethyl)oxane-2-thiolate
triethylphosphane	Caki-1: human clear cell renal cell carcinoma: DPPF: 1,1′-Ferrocenediyl-bis(diphenylphosphine)
DTNB	(5, 5'-dithiobis (2-nitrobenzoic) acid
HCT 116	human colorectal carcinoma
HUVEC	human umbilical vein endothelial cells
ILs	Interleukins
IMes	1,3-bis(2,4,6-trimethylphenyl)imidazole-2-ylidene
IRM90	human foetal lung fibroblast: mba
MMPs	matrix metalloproteinase
NHC	N-heterocyclic carbene
TNB^2	5-thio-2-nitrobenzoic acid

TrRx	thioredoxin reductase
VEGF	vascular endothelial growth factor

References

[1]. Pelletier F, Comte V, Massard A, Wenzel M, Toulot S, Richard P, Picquet M, Le Gendre P, Zava O, Edafe F, et al. Development of Bimetallic Titanocene-Ruthenium-Arene Complexes as Anticancer Agents: Relationships between Structural and Biological Properties. J. Med. Chem 53 (2010) 6923–6933. [PubMed: 20822096]

[2]. Liu Y, Chen T, Wong YS, Mei WJ, Huang XM, Yang F, Liu J, Zheng WJ DNA Bindingand Photocleavage Properties and Apoptosis-Inducing Activities of a Ruthenium Porphyrin Complex [(Py-3')TPP-Ru(phen)2Cl]Cl and Its Heterometallic Derivatives. Chem. Biol. Interact 183 (2010) 349–356. [PubMed: 19958751]

[3]. Wenzel M, Bertrand B, Eymin MJ, Comte V, Harvey JA, Richard P, Groessl M, Zava O, Amrouche H, Harvey PD, et al. Multinuclear Cytotoxic Metallodrugs: Physicochemical Characterization and Biological Properties of Novel Heteronuclear Gold-Titanium Complexes. Inorg. Chem 2011, 50 (19), 9472–9480. [PubMed: 21875041]

[4]. Bjelosevic H, Guzei IA, Spencer LC, Persson T, Kriel FH, Hewer R, Nell MJ, Gut J, van Rensburg CEJ, Rosenthal PJ, et al. Platinum(II) and gold(I) Complexes Based on 1,1′-Bis(diphenylphosphino)metallocene Derivatives: Synthesis, Characterization and Biological Activity of the Gold Complexes. J. Organomet. Chem 720 (2012) 52–59.

[5]. Kaushik NK, Mishra A, Ali A, Adhikari JS, Verma AK, Gupta R Synthesis, Characterization, and Antibacterial and Anticancer Screening of $\{M^{2+}\text{-}Co^{3+}\text{-}M^{2+}\}$ and $\{Co^{3+}\text{-}M^{2+}\}$ (M is Zn, Cd, Hg) Heterometallic Complexes. J. Biol. Inorg. Chem 17 (2012) 1217–1230. [PubMed: 23001051]

[6]. Nieto D, González-Vadillo AM, Bruña S, Pastor CJ, Ríos-Luci C, León LG, Padrón JM, Navarro-Ranninger C, Cuadrado I Heterometallic Platinum(II) Compounds with β-Aminoethylferrocenes: Synthesis, Electrochemical Behaviour and Anticancer Activity. Dalton Trans. 41(2012) 432–441. [PubMed: 22025199]

[7]. Lease N, Vasilevski V, Carreira M, De Almeida A, Sanaú M, Hirva P, Casini A, Contel M Potential Anticancer Heterometallic Fe-Au and Fe-Pd Agents: Initial Mechanistic Insights. J. Med. Chem 56 (2013) 5806–5818. [PubMed: 23786413]

[8]. García-Moreno E, Gascón S, Rodriguez-Yoldi MJ, Cerrada E, Laguna M S -Propargylthiopyridine Phosphane Derivatives as Anticancer Agents: Characterization and Antitumor Activity. Organometallics 32 (2013) 3710–3720.

[9]. Barreiro E, Casas JS, Couce MD, Sánchez A, Sordo J, Vázquez-López EM Heteronuclear gold(I)-silver(I) Sulfanylcarboxylates: Synthesis, Structure and Cytotoxic Activity against Cancer Cell Lines. J. Inorg. Biochem 131 (2014) 68–75. [PubMed: 24269769]

[10]. Wenzel M, Bigaeva E, Richard P, Le Gendre P, Picquet M, Casini A, Bodio E New Heteronuclear gold(I)-platinum(II) Complexes with Cytotoxic Properties: Are Two Metals Better than One? J. Inorg. Biochem 141 (2014) 10–16. [PubMed: 25172993]

[11]. Fernández-Moreira V, Marzo I, Gimeno MC Luminescent Re(i) and Re(i)/Au(i) Complexes as Cooperative Partners in Cell Imaging and Cancer Therapy. Chem. Sci 5 (2014) 4434–4446.

[12]. Zaidi Y, Arjmand F, Zaidi N, Usmani JA, Zubair H, Akhtar K, Hossain M, Shadab GGHA A Comprehensive Biological Insight of Trinuclear Copper(II)–tin(IV) Chemotherapeutic Anticancer Drug Entity: In Vitro Cytotoxicity and in Vivo Systemic Toxicity Studies. Metallomics 6 (2014) 1469–1479. [PubMed: 24817323]

[13]. Govender P, Lemmerhirt H, Huttonm AT, Therrien B, Bednarski PJ, Smith GS First-and Second-Generation Heterometallic Dendrimers Containing Ferrocenyl-ruthenium(II)-Arene Motifs: Synthesis, Structure, Electrochemistry, and Preliminary Cell Proliferation Studies. Organometallics 33 (2014) 5535–5545.

[14]. Bertrand B, Citta A, Franken IL, Picquet M, Folda A, Scalcon V, Rigobello MP, Le Gendre P, Casini A, Bodio E Gold(I) NHC-Based Homo- and Heterobimetallic Complexes: Synthesis,

Characterization and Evaluation as Potential Anticancer Agents. J. Biol. Inorg. Chem 2015, 20 (6), 1005–1020. [PubMed: 26202908]

[15]. Boselli L, Carraz M, Mazères S, Paloque L, González G, Benoit-Vical F, Valentin A, Hemmert C, Gornitzka H Synthesis, Structures, and Biological Studies of Heterobimetallic Au(I)-Ru(II) Complexes Involving N-Heterocyclic Carbene-Based Multidentate Ligands. Organometallics 34 (2015) 1046–1055.

[16]. Nieto D, Bruña S, González-Vadillo AM, Perles J, Carrillo-Hermosilla F, Antiñolo A, Padrón JM, Plata GB, Cuadrado I Catalytically Generated Ferrocene-Containing Guanidines as Efficient Precursors for New Redox-Active Heterometallic Platinum(II) Complexes with Anticancer Activity. Organometallics 34 (2015) 5407–5417.

[17]. Nithyakumar A, Alexander V Synthesis, Relaxivity, and in Vitro Fluorescence Imaging Studies of a Novel d–f Heterometallic Trinuclear Complex as a Potential Bimodal Imaging Probe for MRI and Optical Imaging. Dalton Trans. 44 (2015) 17800–17809. [PubMed: 26400754]

[18]. Fenton JM, Busse M, Rendina LM Synthesis and DNA-Binding Studies of a Dinuclear Gadolinium(iii)–Platinum(ii) Complex. Aust. J. Chem 68 (2015) 576–580.

[19]. Ma L, Ma R, Wang Z, Yiu S-M, Zhu G Heterodinuclear Pt(IV)–Ru(II) Anticancer Prodrugs to Combat Both Drug Resistance and Tumor Metastasis. Chem. Commun 52 (2016) 10735–10738.

[20]. Singh N, Jang S, Jo JH, Kim DH, Park DW, Kim IH, Kim IH, Kang SC, Chi KW Coordination-Driven Self-Assembly and Anticancer Potency Studies of Ruthenium–Cobalt-Based Heterometallic Rectangles. Chem. - A Eur. J 22 (2016) 16157–16164.

[21]. Lopes J, Alves D, Morais TS, Costa PJ, Piedade MFM, Marques F, Villa de Brito MJ, Helena Garcia M New copper(I) and Heteronuclear copper(I)–ruthenium(II) Complexes: Synthesis, Structural Characterization and Cytotoxicity. J. Inorg. Biochem 169 (2017) 68–78. [PubMed: 28142080]

[22]. Luengo A, Fernández-Moreira V, Marzo I, Gimeno MC Trackable Metallodrugs Combining Luminescent Re(I) and Bioactive Au(I) Fragments. Inorg. Chem 56 (2017) 15159–15170. [PubMed: 29172469]

[23]. Ma L, Lin X, Li C, Xu Z, Chan C-Y, Tse M-K, Shi P, Zhu G A cancer cell-selective and low-toxic bifunctional heterodinuclear Pt(IV)-Ru(II) anticancer prodrug. Inorg. Chem 57 (2018) 2917–2924. [PubMed: 29436828]

[24]. González-Pantoja JF, Stern M, Jarzecki AA, Royo E, Robles-Escajeda E, Varela-Ramírez A, Aguilera RJ, Contel M Titanocene-Phosphine Derivatives as Precursors to Cytotoxic Heterometallic TiAu 2 and TiM (M = Pd, Pt) Compounds. Studies of Their Interactions with DNA. Inorg. Chem 50 (2011) 11099–11110. [PubMed: 21958150]

[25]. Fernández-Gallardo J, Elie BT, Sulzmaier FJ, Sanaú M, Ramos JW, Contel M Organometallic Titanocene-Gold Compounds as Potential Chemotherapeutics in Renal Cancer. Study of Their Protein Kinase Inhibitory Properties. Organometallics 33 (2014) 6669–6681. [PubMed: 25435644]

[26]. (a) Fernández-Gallardo J, Elie BT, Sadhukha T, Prabha S, Sanaú M, Rotenberg S, Ramos JW, Contel M Heterometallic Titanium–gold Complexes Inhibit Renal Cancer Cells in Vitro and in Vivo. Chem. Sci 6 (2015) 5269–5283. [PubMed: 27213034] (b) Contel M, Fernández-Gallardo J, Elie BT, Ramos JW US Patent 9,315,531 (04/19/2016).

[27]. Mui YF, Fernández-Gallardo J, Elie BT, Gubran A, Maluenda I, Sanaú M, Navarro O, Contel M Titanocene-Gold Complexes Containing N-Heterocyclic Carbene Ligands Inhibit Growth of Prostate, Renal, and Colon Cancers in Vitro. Organometallics 35 (2016) 1218–1227. [PubMed: 27182101]

[28]. Massai L, Fernández-Gallardo J, Guerri A, Arcangeli A, Pillozzi S, Contel M, Messori L Design, Synthesis and Characterisation of New Chimeric Ruthenium(II)–gold(I) Complexes as Improved Cytotoxic Agents. Dalton Trans. 44 (2015) 11067–11076. [PubMed: 25996553]

[29]. Fernández-Gallardo J, Elie BT, Sanaú M, Contel M Versatile Synthesis of Cationic N-Heterocyclic Carbene–gold(I) Complexes Containing a Second Ancillary Ligand. Design of Heterobimetallic Ruthenium–gold Anticancer Agents. Chem. Commun 52 (2016) 3155–3158.

[30]. Elie BT, Pechenyy Y, Uddin F, Contel M A heterometallic ruthenium-gold complex displays antiproliferative, antimigratory and antiangiogenic properties and inhibits metastasis and

angiogenesis-associated proteases in renal cancer. J. Biol. Inorg. Chem 23 (2018) 399–411. [PubMed: 29508136]

[31]. Benoît B, Casini A A golden future in medicinal inorganic chemistry: the promise of anticancer gold organometallic compounds. Dalton Trans. 43 (2014) 4209–4219 and refs. therein. [PubMed: 24225667]

[32]. Owings JP, McNair NN, Mui YF, Gustafsson TN, Holmgren A, Contel M, Goldberg JB, Mead JR Auranofin and *N*-heterocyclic carbene gold-analogs are potent inhibitors of the bacteria *Helicobacter pylory*. FEMS Microbiology Letters 363 (2016) fnw148 and refs. therein.

[33]. Marzo T, Cirri D, Gabbiani C, Gamberi T, Magherini F, Pratesi A, Guerri A, Biver T, Binacchi F, Stefanini M, Arcangeli M;A, Messori L Auranofin, Et_3PAuCl, and Et_3PAuI Are Highly Cytotoxic on Colorectal Cancer Cells: A Chemical and Biological Study. ACS Med. Chem. Lett 8 (2017) 997–1001. [PubMed: 29057040]

[34]. Shaw CF Gold-based therapeutic agents. Chem. Rev 99, 1999, 2589–2600. [PubMed: 11749494]

[35]. Roder C, Thomson M Auranofin: Repurposing an old drug for a golden new age. Drugs in R&D, 15 (2015) 13–20 and refs. therein. [PubMed: 25698589]

[36]. Phase I and II study of Auranofin in Chronic Lymphocytic Leukemia (CLL)'. https://clinicaltrials.gov/ct2/show/NCT01419691.

[37]. 'PKCi & mTOR Inhibition With Auranofin+Sirolimus for Squamous Cell Lung Cancer'. https://clinicaltrials.gov/ct2/show/NCT01737502.

[38]. 'Auranofin in Treating Patients With Recurrent Epithelial Ovarian, Primary Peritoneal, or Fallopian Tube Cancer'. https://clinicaltrials.gov/ct2/show/NCT01747798.

[39]. Dean TC, Yang M Liu M, Grayson JM, DeMartino AW, Day CS, Lee J, Furdui CM, Bierbach U Human Serum Albumin-Delivered [Au(PEt3)]+ Is a Potent Inhibitor of T Cell Proliferation. ACS Med. Chem. Lett 8 (2017) 572–576. [PubMed: 28523113]

[40]. Schmidbaur H, Cronje S, Djordjevic B, Schuster O Understanding gold chemistry through relativity. Chem. Phys 311 (2015) 151–161.

[41]. Tiekink ERT Supramolecular assembly of molecular gold(I) compounds: An evaluation of the competition and complementarity between aurophilic (Au···Au) and conventional hydrogen bonding interactions. Coord. Chem. Rev 275 (2014) 130–153.

[42]. O'Connor K, Gill C, Tacke M, Rehmann F-JK, Strohfeldt K, Sweeney N, Fitzpatrick JM, Watson RWG Novel titanocene anti-cancer drugs and their effect on apoptosis and the apoptotic pathway in prostate cancer cells. Apoptosis, 11 (2016) 1205–1214.

[43]. Nakaya A, Sagawa M, Muto A, Uchida H, Ikeda Y, Kizaki M The gold compound auranofin induces apoptosis of human multiple myeloma cells through both down-regulation of STAT3 and inhibition of NF-κB activity. Leukemia Res. 35 (2011) 243–249. [PubMed: 20542334]

[44]. Fan C, Zheng W, Fu X, Li X, Wong YS, Chen T Enhancement of auranofin-induced lung cancer cell apoptosis by selenocystine, a natural inhibitor of TrxR1 in vitro and in vivo. Cell Death Dis. 5 (2014) e1191. [PubMed: 24763048]

[45]. Varghese E, Büsselberg D Auranofin, an Anti-Rheumatic Gold Compound, Modulates Apoptosis by Elevating the Intracellular Calcium Concentration ([Ca2+]i) in MCF-7 Breast Cancer Cells. Cancers, 6 (2014) 2243–2258. [PubMed: 25383481]

[46]. Sagawa M, Nakaya A, Tomikawa T, Haba Y, Nemoto T, Hanzawa K, Watanabe R, Tokuhira M, Mori S, Uchida H, Muto A, Kizaki M Gold Compound Auranofin (RIDAURA®) Induces Apoptosis of Human Myeloma Cells by Targeting STAT3 and NF-κB Pathways, with Clinical Potential. Blood, 114 (2009) 3831–3837. [PubMed: 19704119]

[47]. Pessetto ZY, Weir SJ, Sethi G, Broward MA, Godwin AK Drug repurposing for gastrointestinal stromal tumor. Mol. Cancer Ther 12 (2013) 1299–1309. [PubMed: 23657945]

[48]. Kim NH, Lee MY, Park SJ, Choi JS, Oh MK, Kim IS Auranofin blocks interleukin-6 signaling by inhibiting phosphorylation of JAK1 and STAT3. Immunology, 122 (2007) 607–614. [PubMed: 17645497]

[49]. Rayburn ER, Scharri SJ, Zhang R Anti-inflammatory agents for cancer therapy. Mol. Cell. Pharmacol 1 (2009) 29–43. [PubMed: 20333321]

[50]. Ray MR, Jablons DM Hallmarks of Metastasis In: Keshamouni V, Arenberg D, Kalemkerian G (eds) Lung Cancer Metastasis. Springer, New York, NY, 2009.

[51]. Zhang W, Kai K, Ueno NT, Quin L, et al. A Brief Review of the Biophysical Hallmarks of Metastatic Cancer Cells. Cancer Hallm. 1 (2013) 59–66. [PubMed: 25309822]

[52]. DeCicco-Skinner KL, Henry GH, Cataisson C, Tabib T, Gwilliam JC, Watson NJ, Bullwinkle EM, Falkenburg L, O'Neill RC, Morin A, Wiest JS Endothelial cell tube formation assay for the in vitro study of angiogenesis. J. Vis. Exp (2014) 91:e51312.

[53]. Streicher KL, Sylte MJ, Johnson SE, Sordillo LM Thioredoxin reductase regulates angiogenesis by increasing endothelial cell-derived vascular endothelial growth factor. Nutr. Cancer. 50 (2014) 221–231.

[54]. Chen C, Li L, Zhou HJ, Min W The Role of NOX4 and TRX2 in Angiogenesis and Their Potential Cross-Talk. Antioxidants, 6 (2017) pii:E42. [PubMed: 28594389]

[55]. Karlenius TC, Tonissen KF Thioredoxin and cancer: a role for thioredoxin in all states of tumor oxygenation. Cancers, 2 (2010), 209–232. [PubMed: 24281068]

[56]. Wang P, Wu Y, Li X, Ma X, Zhong L Thioredoxin and thioredoxin reductase control tissue factor activity by thiol redox-dependent mechanism. J. Biol. Chem 288 (2013) 3346–3358. [PubMed: 23223577]

[57]. López-Ocejo O, Viloria-Petit A, Bequet-Romero M, Mukhopadhyay D, Rak J, Kerbel RS Oncogenes and tumor angiogenesis: The HPV-16 E6 oncoprotein activates the vascular endothelial growth factor (VEGF) gene promoter in a p53 independent manner. Oncogene, 19 (2000) 4611–4620. [PubMed: 11030150]

[58]. Rak J, Mitsuhashi Y, Sheehan C, Tamir A, Viloria-Petit A, Filmus J, Mansour SJ, Ahn NG, Kerbel RS Oncogenes and tumor angiogenesis: differential modes of vascular endothelial growth factor up-regulation in ras-transformed epithelial cells and fibroblasts. Cancer Res. 60 (2000) 490–498. [PubMed: 10667605]

[59]. Roskoski R, Jr. Vascular endothelial growth factor (VEGF) signaling in tumor progression. Crit. Rev. Oncol. Hematol 62 (2007) 179–213. [PubMed: 17324579]

[60]. Bergers G, Benjamin LE Tumorigenesis and the angiogenic switch. Nat. Rev. Cancer, 3 (2003) 401–410. [PubMed: 12778130]

[61]. Wang X, Lin Y Tumor necrosis factor and cancer, buddies or foes? Acta Pharmacol. Sin 29 (2008) 1275–1288. [PubMed: 18954521]

[62]. Shi G, Zheng X, Zhang S, Wu X, Yu F, Wang Y, Xing F Kanglaite inhibits EMT caused by TNF-α via NF-κB inhibition in colorectal cancer cells. Oncotarget 9 (2018) 6771–6779. [PubMed: 29467927]

[63]. Aggarwal BB Signaling pathways of the TNF superfamily: a double-edged sword. Nat. Rev. Immunol 3 (2003) 745–756. [PubMed: 12949498]

[64]. Hallett MA, Venmar KT, Fingleton B Cytokine stimulation of epithelial cancer cells: the similar and divergent functions of IL4 and IL13. Cancer Res. 72 (2012) 6338–6343. [PubMed: 23222300]

[65]. Todaro M, Lombardo Y, Francipane MG, Alea MP, Cammareri P, Iovino F, Di Stefano AB, Di Bernardo C, Agrusa A, Condorelli G, Walczak H, Stassi G Apoptosis resistance in epithelial tumors is mediated by tumor-cell-derived interleukin-4. Cell Death Differ. 15 (2018) 762–72.

[66]. Landskron G, De la Fuente M, Thuwajit P, Thuwajit C, Hermoso MA Chronic inflammation and cytokines in the tumor microenvironment. J. Immunol Res (2014) 2014:149185. [PubMed: 24901008]

[67]. Jiang YN, Yan HQ, Huang XB, Wang YN, Li Q, Gao FG Interleukin 6 trigged ataxia-telangiectasia mutated activation facilitates lung cancer metastasis via MMP-3/MMP-13 up-regulation. Oncotarget, 6 (2015) 40719–40733. [PubMed: 26528698]

[68]. Gialeli C, Theocharis AD, Karamanos NK Roles of matrix metalloproteinases in cancer progression and their pharmacological targeting. FEBS J. 278 (2011) 16–27. [PubMed: 21087457]

[69]. Cathcart J, Pulkoski-Gross A, Cao J Targeting Matrix Metalloproteinases in Cancer: Bringing New Life to Old Ideas. Genes Dis. 2 (2015) 26–34. [PubMed: 26097889]

[70]. Coussens LM, Fingleton B, Matrisian LM Matrix metalloproteinase inhibitors and cancer: trials and tribulations. Science 295 (2002) 2387–2392. [PubMed: 11923519]

[71]. Amar S, Fields GB Potential clinical implications of recent MMP inhibitor design strategies. Expert review of proteomics, 12 (2015) 445–447. [PubMed: 26174966]

[72]. Leifler KS, Svensson S, Abrahamsson A, Bendrik C, Robertson J, Gauldie J, Olsson AK, Dabrosin C Inflammation Induced by MMP-9 Enhances Tumor Regression of Experimental Breast Cancer. J. Immunol 190 (2013) 4420–4430. [PubMed: 23509357]

[73]. Yousef EM, Tahir MR, St-Pierre Y, Gaboury LA MMP-9 expression varies according to molecular subtypes of breast cancer. BMC Cancer, (2014) 14:609. [PubMed: 25151367]

[74]. Westbrook JA, Caims DA, Peng J, Speirs V, Hanby AM, Holen I, Wood SL, Ottewell PD, Masrshall H, Banks RE, Selby PJ, Coleman RE, Brown JE CAPG and gipc1: Breast cancer biomarkers for bone metastasis development and treatment. J. Natl. Cancer Inst 108 (2016) djv360.

[75]. Watari A, Takaki K, Higashiyama S, Li Y, Satomi Y, Takao T, Tanemura A, Yamaguchi Y, Shimakage M, Miyashiro I, Takami K, Kodama K, Yutsudo M Suppression of tumorigenicity, but not anchorage independence, of human cancer cells by new candidate tumor suppressor gene CapG. Oncogene, 25 (2006) 7373–7380. [PubMed: 16767159]

[76]. Swiercz JM, Worzfeld T, Offermanns S ErbB-2 and Met Reciprocally Regulate Cellular Signaling via Plexin-B1. J. Biol. Chem 283 (2018) 1893–1901.

[77]. Korc M, Friesel RE The role of fibroblast growth factors in tumor growth. Curr. Cancer Drug Targets, 9 (2009) 639–51. [PubMed: 19508171]

[78]. Hu M, Hu Y, He J, Li B Prognostic value of basic fibroblast growth factor (bFGF) in lung cancer: A systematic review with meta-analysis. PLoS ONE (2016) doi:10.1371/journal.pone.0147374.

[79]. Kalluri R The biology and function of fibroblasts in cancer. Nat. Rev. Cancer, 16 (2016), 582–598. [PubMed: 27550820]

[80]. Paranjape AN, Soundararajan R, Werden SJ, Josephm R, Taube JH, Liu H, Rodriguez-Canales J, Sphyris N, Wistuba I, Miura N, Dhillon J, Mahajan N, Mahajan K, Chang JT, Ittmann M, Maity SN, Logothetis C, Tang DG, Mani SA Inhibition of FOXC2 restores epithelial phenotype and drug sensitivity in prostate cancer cells with stem-cell properties. Oncogene, 17 (2016) 5963–5976.

[81]. Kume T The role of FoxC2 transcription factor in tumor angiogenesis. J. Oncol (2012) article ID 204593.

[82]. DeLisser HM Targeting PECAM-1 for anti-cancer therapy. Cancer Biol. Ther 6 (2007) 121–122. [PubMed: 17297300]

[83]. Cui SY, Huang JY, Chen YT, Song HZ, Huang GC, De W, Wang R, Chen LB The role of Aurora A in hypoxia-inducible factor 1α-promoting malignant phenotypes of hepatocelluar carcinoma. Cell Cycle 12 (2013) 2849–2866. [PubMed: 23966163]

[84]. Masoud GN, Li W HIF-1α pathway: Role, regulation and intervention for cancer therapy. Acta Pharm. Sin. B 5 (2015) 378–389. [PubMed: 26579469]

[85]. Shen H, Hau E, Joshi S, Dilda PJ, McDonald KL Sensitization of Glioblastoma Cells to Irradiation by Modulating the Glucose Metabolism. Mol Cancer Ther 14 (2015) 1794–804. [PubMed: 26063767]

[86]. Yoshida T, Akatsuka T, Imanaka-Yoshida K Tenascin-C and integrins in cancer. Cell Adh. Migr 9 (2015) 96–104. [PubMed: 25793576]

[87]. Lowy CM, Oskarsson T Tenascin C in metastasis: A view from the invasive front. Cell Adh. Migr 9 (2015) 112–124. [PubMed: 25738825]

[88]. Oskarsson T, Acharyya S, Zhang XH-F, Vanharanta S, Tavazoie SF, Morries PG, Downey RJ, Manova-Todoriva K, Brogi E, Massagué J Breast cancer cells produce tenascin C as a metastatic niche component to colonize the lungs. Nat. Med 17 (2011) 867–864. [PubMed: 21706029]

[89]. Payack JF, Hughes DL, Cai D, Cottrell IF, Verhoeven TR Dimethyltitanocene. Org. Synth 79 (2002) 19.

Highlights

- Synthesis of an Auranofin-analogue containing titanocene active against renal cancer
- Mechanistic studies on two titanocene-gold compounds, and Auranofin in renal cancer Caki-1 cells
- Bimetallic compounds highly cytotoxic (nanomolar range), selective and apoptotic
- Relevant inhibition of migration, invasion, and angiogenic assembly
- Inhibition of molecular markers associated with the processes described above

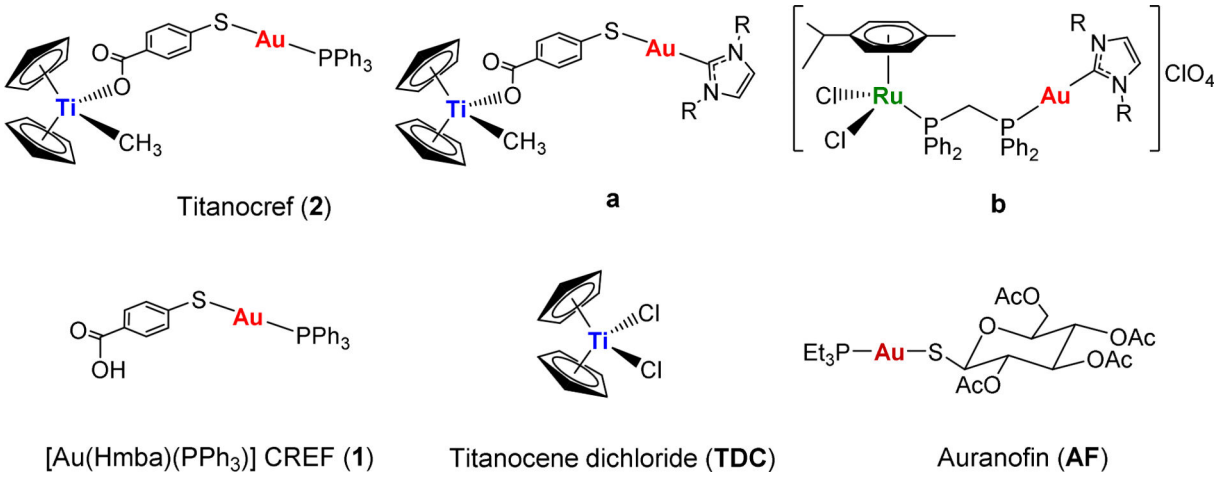

Chart 1.

Select heterometallic Ti-Au (2, a) and Ru-Au (b) compounds with relevant in vitro and in vivo activity reported by our group [26,27,29,30]. Structure of monometallic [Au(Hmba)(PPh3)] (1), Auranofin (AF) and Titanocene dichloride (TDC) also employed in this work.

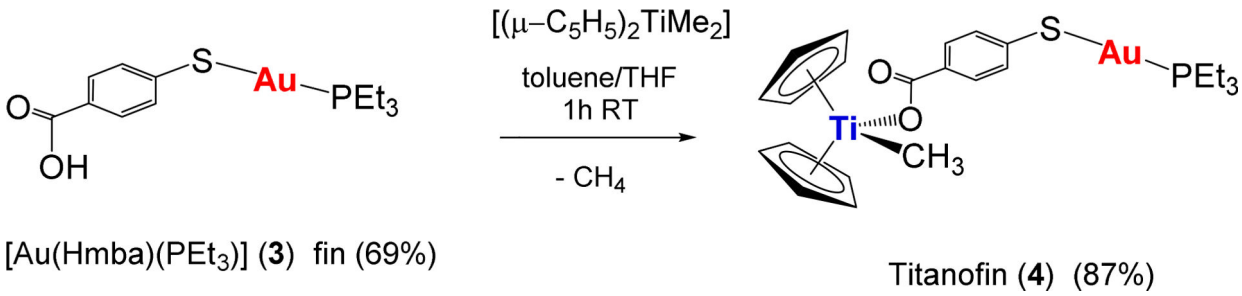

Equation 1.
Preparation of [(η-C_5H_5)$_2$TiMe(μ-mba)Au(PEt_3)] (**4**) Titanofin.

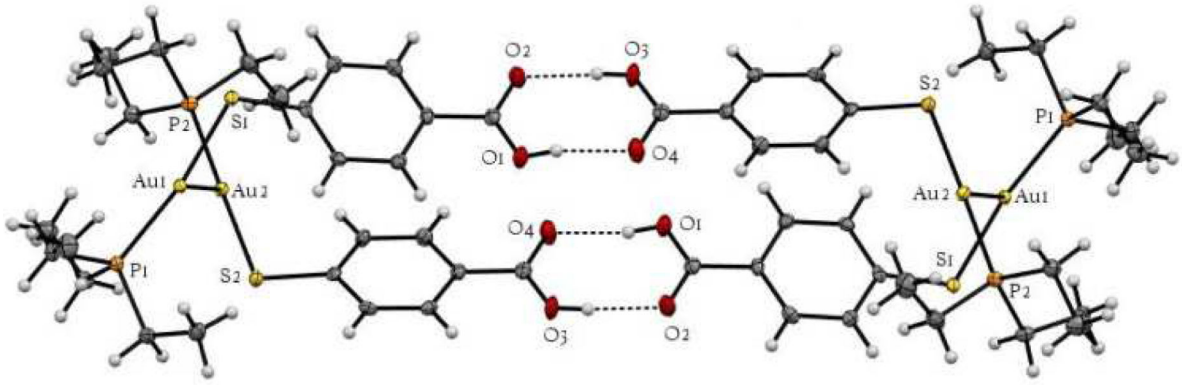

Figure 1.

ORTEP view of the polymeric structure of **3** showing hydrogen bonds (blue dotted line) and the Au-Au interactions.

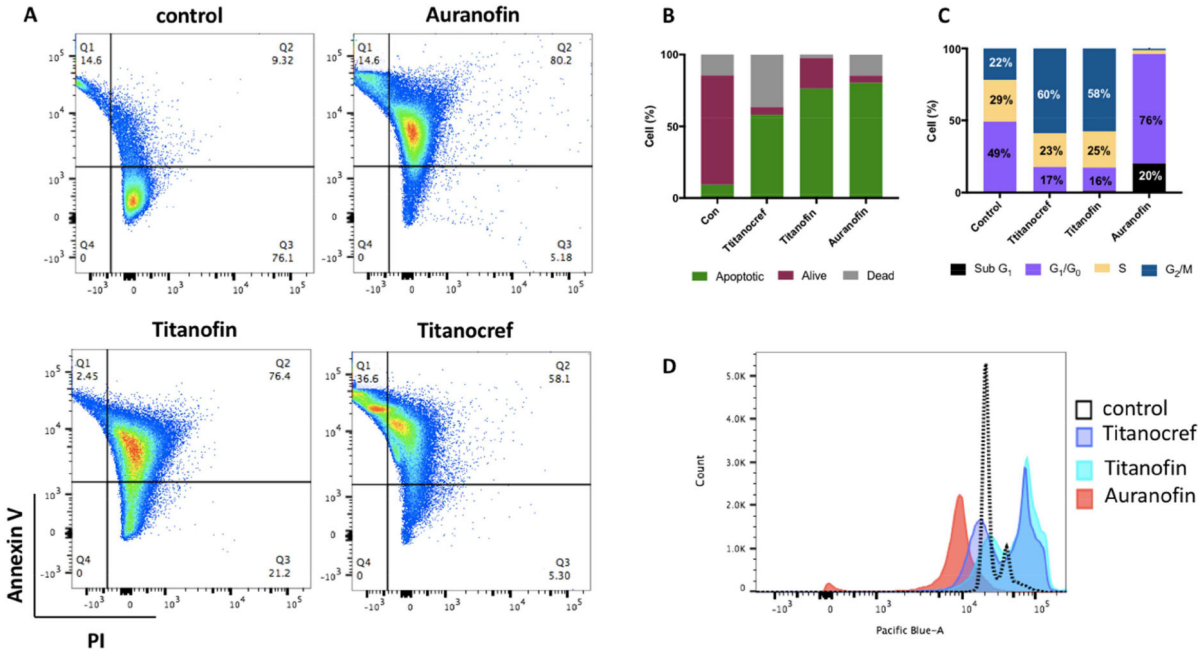

Figure 2.

Effects of Titanocref (**2**), Titanofin (**4**) and Auranofin on apoptotic index and cell cycle distribution on Caki-1 cells. (A) Cell apoptosis in bimetallic Titanocref (**2**), Titanofin (**4**) and monometallic Auranofin treated cells was detected by Annexin V and propidium iodide (PI) labeling detected by flow cytometry after 72h of incubation with IC_{50}. The extent of apoptosis was determined by the percentage of the total cells that were positive for PI reported in each quadrant 2 (Q1= dead cells, Q2=Apoptotic cells, Q3= Alive cells). Treatment with of bimetallic Titanocref (**2**), Titanofin (**4**) and monometallic Auranofin for 24h caused cell cycle arrest. Cell-cycle analysis was conducted by FxCycle staining and flow cytometry 24 h after treatment with bimetallic Titanocref (**2**), Titanofin (**4**), monometallic Auranofin or DMSO (0.1%) control. Numbers in the bar-graph (C) correspond to histograms (D) indicate the percentage of cells in the Sub G_1, G_0-G_1, S and G_2-M phases of the cell cycle (values below 3% were not reported on the bar-graph).

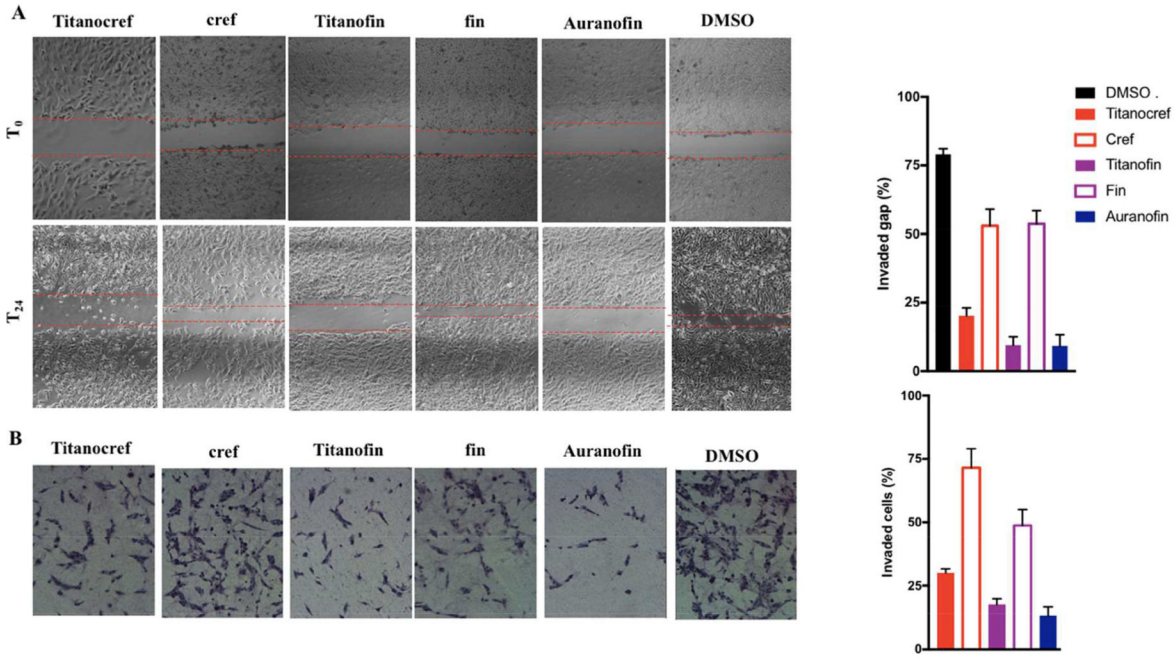

Figure 3.

Cell Migration and Invasion Inhibition Assays for bimetallic Ti-Au Titanocref (**2**), Titanofin (**4**) and monometallic Au cref (**2**), fin (**3**) and Auranofin. **A.** Inhibition of migration (2D wound-healing scratch assay). Scratch assay showing that Titanocref (**2**), Titanofin (**4**) and monometallic Au cref (**2**), fin (**3**) and Auranofin interfere with Caki-1 migration. Panels show representative images of untreated cells at time points T_0 (top row) when the compound is added to the assay up to 24 hours (bottom row). **B.** Inhibition of invasion (3D transwell assay Geltrex) showing that Titanocref (**2**), Titanofin (**4**) and monometallic Au cref (**2**), fin (**3**) and Auranofin interfere with Caki-1 invasion. The values graphed are normalized to DMSO control. The invasion assay was performed using an ECM-like Reduced Growth Factor Basement Membrane Matrix (Geltrex) 3:1. Panels show representative images of cells 24 hours after treatment with the 72h IC_{20} concentration at which we observe less than 8% cell death after 24h of incubation. The data reported in the graph, and standard deviation of the sample mean, result from two independent trials averaging quantitation from five fields of view per trial.

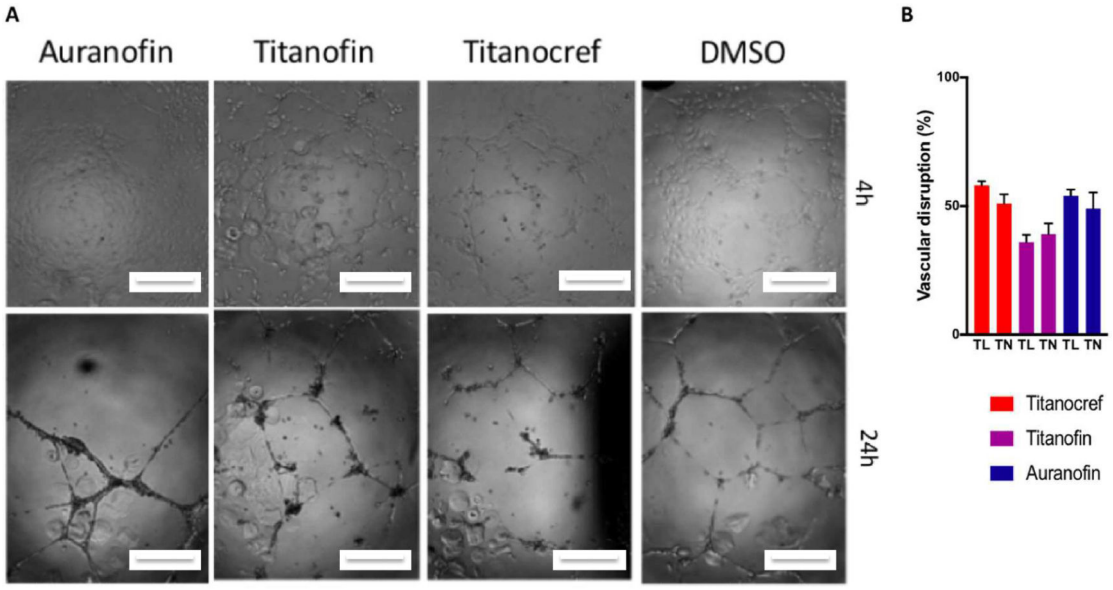

Figure 4.

Effects on vascular endothelial cell reorganization into 3D structures. Human umbilical vein endothelial cells (HUVEC) were seeded with the appropriate media in plates coated with Geltrex® matrix and incubated at 37°C and 5% CO_2. Thereafter, the 72h IC_{10} of bimetallic Ti-Au Titanocref (**2**), Titanofin (**4**) and Auranofin or 0.1% DMSO was added. (A) Representative phase-contrast images captured 4h then 24h post dosing. Scale bar = 100 μm. (B) Quantitation of tube formation was performed using Image-J with the Angiogenesis plugin. The data reported in the graph, and standard deviation of the sample mean, result from two independent trials averaging quantitation from five fields of view per trial.

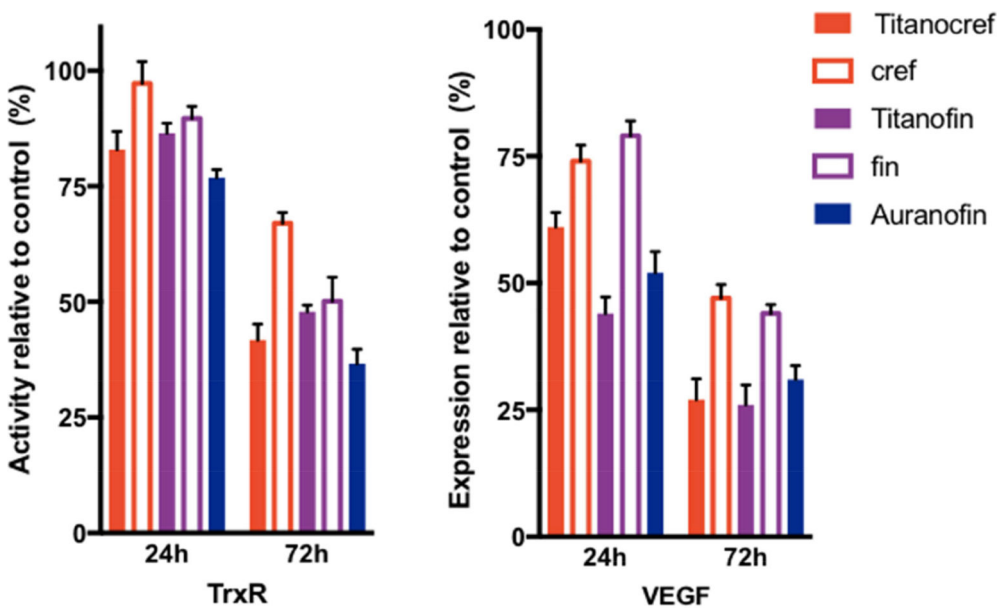

Figure 5.

Inhibition of proangiogenic factors TrxR and VEGF in Caki-1 cells by bimetallic Ti-Au Titanocref (**2**), Titanofin (**4**) and monometallic Au cref (**2**), fin (**3**) and Auranofin occurs in a time and dose dependent manner. **A**. inhibition of proangiogenic anti-apoptotic mitochondrial protein TrxR following treatment with IC_{20} concentrations of each compound for 24 h and 72h. The values indicate the percentage of TrxR activity relative to DMSO treated cells. **B**. Inhibition of proangiogenic protein VEGF, following treatment with IC_{20} concentrations of each compound for 24 h and 72h. The values indicate the percentage of VEGF expression relative to DMSO treated cells. Analysis of 150 ng of protein extracted from cell lysate. The data shown, and standard deviation of the sample mean, result from two independent trials.

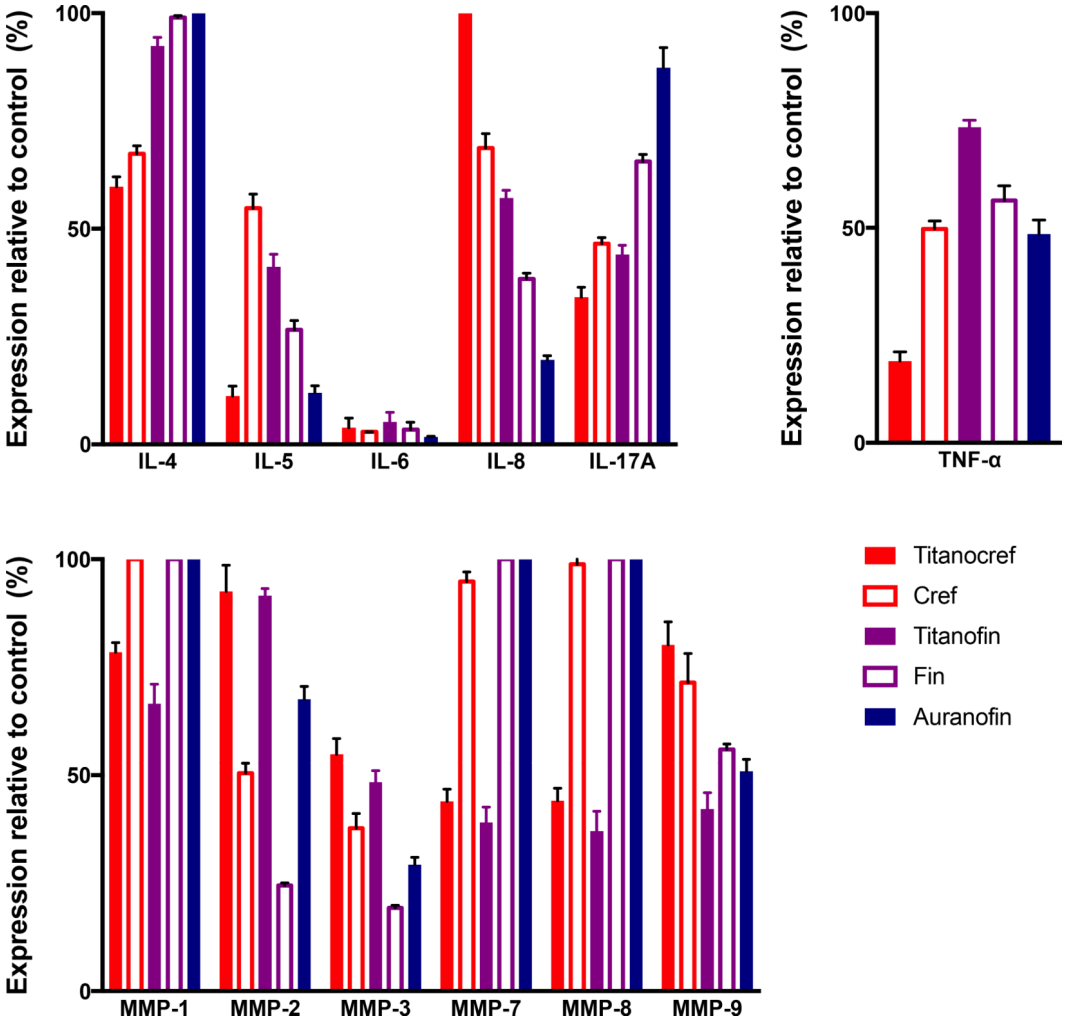

Figure 6.

Bimetallic Ti-Au Titanocref (**2**), Titanofin (**4**) and monometallic Au cref (**2**), fin (**3**) and Auranofin induced changes in the expression levels of prometastatic cytokines (TNF-α, and interleukins) and matrix proteases (MMMPs -matrix metalloproteinases) in Caki-1 cells. Analysis of 150 ng of protein extracted from cell lysate collected from cell treated with IC_{20} of the compounds for 72h. The data shown, and standard deviation of the sample mean, result from two independent trials.

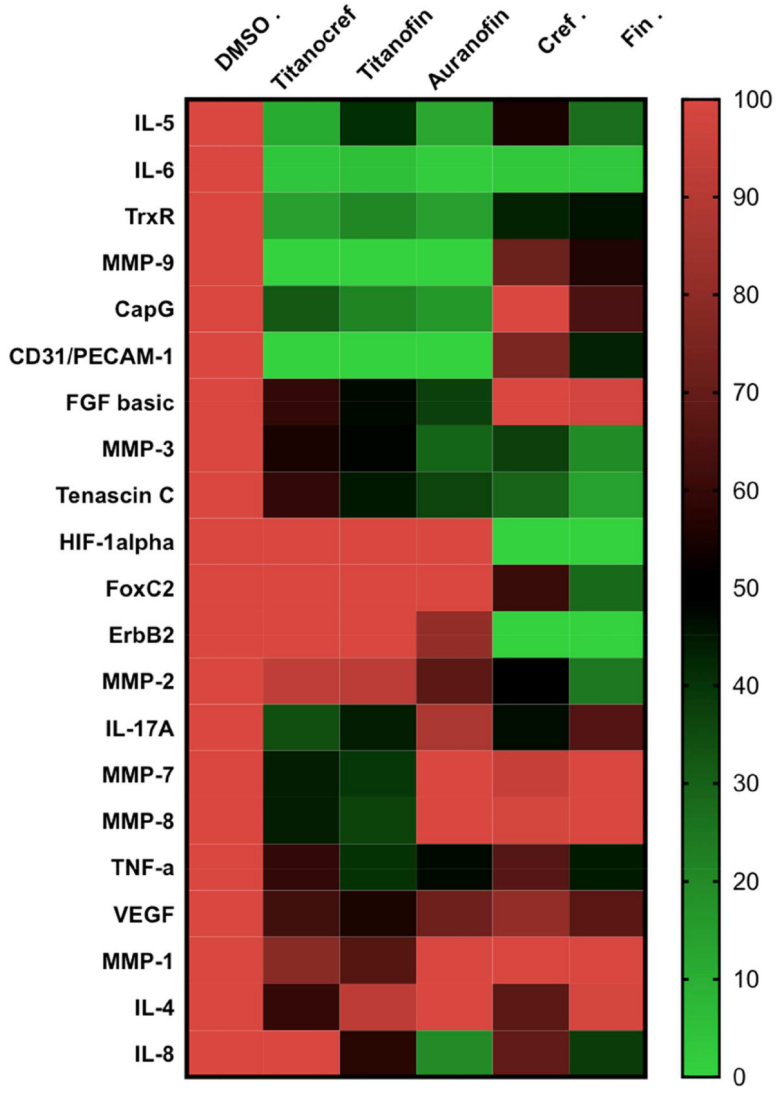

Figure 7.

Heat map visualization of protein expression data. Each row represents a protein of oncological interest and each column represents a specific compound incubated for 72h at IC_{20}. Markers features whose levels vary significantly ($p < 0.05$) between at least two treatment groups are projected on the heat map and used for drug response clustering. Analysis of 150 ng of protein extracted from cell lysate collected from bimetallic Titanocref **2** and Titanofin **4**, monometallic cref **1**, fin **3** and Auranofin treated cells is IC_{20}. Relative expression value of each protein interrogated is plotted in red-green color scale. The red color of the tile indicates high abundance and green indicates low abundance. The color gradients indicate the degree of expression relative to the DMSO control. The data shown result from two independent trials.

Table 1.

Selected Structural Parameters of complex **3** obtained from X-ray single crystal diffraction studies. Bond lengths in Å and angles in °.

Au(1)-Au(2)	3.0678(4)	Au(2)-Au(1)-P(1)	97.83(2)
Au(1)-P(1)	2.2707(9)	Au(2)-Au(1)-S(1)	88.91(2)
Au(1)-S(1)	2.3168(8)	P(1)-Au(1)-S(1)	170.17(3)
Au(2)-P(2)	2.2694(8)	Au(1)-Au(1)-P(2)	106.24(2)
Au(2)-S(2)	2.3316(8)	Au(1)-Au(1)-S(2)	76.43(2)
P(1)-C(15)	1.832(3)	P(2)-Au(2)-S(2)	177.32(3)
P(1)-C(17)	1.827(3)	Au(1)-P(1)-C(15)	115.3(1)
P(1)-C(19)	1.821(4)	Au(1)-P(1)-C(17)	115.9(1)
P(2)-C(21)	1.815(3)	Au(1)-P(1)-C(19)	111.6(1)
P(2)-C(23)	1.822(4)	C(15)-P(1)-C(17)	102.5(1)
P(2)-C(25)	1.825(3)	Au(2)-P(2)-C(21)	115.8(1)
S(1)-C(1)	1.766(4)	Au(2)-P(2)-C(23)	112.0(1)
S(2)-C(8)	1.760(4)	Au(2)-P(2)-C(25)	113.6(1)
H(10)-O(4’)	1.809(2)		
O(2)-H(30’)	1.799(4)		

Table 2.

Cell viability IC_{50} values (μM) for Caki-1 cells and IMR-90 fibroblasts treated with bimetallic Titanocref (**2**), Titanofin (**4**) and monometallic gold cref (**1**) and fin (**3**) compounds. Monometallics Auranofin (AF) and titanocene dichloride (TDC) were used as controls.[a] The IC_{50} are reported with the standard deviation of the sample mean.

Compound			Caki-1	IMR90
Ti-Au (PPh_3)	**2**	Titanocref	0.097 ± 0.019	1.6 ± 0.006
[Au(Hmba)(PPh_3)]	**1**	cref	2.70 ± 0.052	3.99 ± 0.09
Ti-Au (PEt_3)	**4**	Titanofin	0.273 ± 0.043	3.131 ± 0.07
[Au(Hmba)(PEt_3)]	**3**	fin	0.794 ± 0.002	2.991 ± 0.006
[Au(SR)(PEt_3)]	**AF**	Auranofin	2.8 ± 0.6[b]	3.7 ± 0.4[b]
$[Ti(Cp)_2Cl_2]$	**TDC**	Titanocene dichloride	>100	>100

[a]All compounds were dissolved in 1% of DMSO and diluted with media before addition to cell culture medium for a 72 hour incubation period. Cisplatin was dissolved in H_2O. Structures of the compounds are provided in Chart 1.

[b]Values reported in reference 30.